The AAPS Journal, Vol. 17, No. 3, May 2015 (© 2015)
DOI: 10.1208/s12248-015-9728-6

Research Article

Mesenchymal Stromal/Stem Cell and Minocycline-Loaded Hydrogels Inhibit the Growth of *Staphylococcus aureus* that Evades Immunomodulation of Blood-Derived Leukocytes

Alberto Daniel Guerra,[1] David Antonio Cantu,[1,2] Joseph T. Vecchi,[2] Warren E. Rose,[1] Peiman Hematti,[3,5] and Weiyuan John Kao[1,2,4,5,6]

Received 25 November 2014; accepted 28 January 2015; published online 26 February 2015

Abstract. Mesenchymal stromal/stem cells (MSCs) have demonstrated favorable wound healing properties in addition to their differentiation capacity. MSCs encapsulated in biomaterials such as gelatin and polyethylene glycol (PEG) composite hydrogels have displayed an immunophenotype change that leads to the release of cytokines and growth factors to accelerate wound healing. However, therapeutic potential of implanted MSC-loaded hydrogels may be limited by non-specific protein adsorption that facilitates adhesion of bacterial pathogens such as planktonic *Staphylococcus aureus* (SA) to the surface with subsequent biofilm formation resistant to immune cell recognition and antibiotic activity. In this study, we demonstrate that blood-derived primary leukocytes and bone marrow-derived MSCs cannot inhibit colony-forming abilities of planktonic or biofilm-associated SA. However, we show that hydrogels loaded with MSCs and minocycline significantly inhibit colony-forming abilities of planktonic SA while maintaining MSC viability and multipotency. Our results suggest that minocycline and MSC-loaded hydrogels may decrease the bioburden of SA at implant sites in wounds, and may improve the wound healing capabilities of MSC-loaded hydrogels.

KEY WORDS: hydrogel; leukocytes; mesenchymal stromal/stem cells; minocycline; *Staphylococcus aureus*.

INTRODUCTION

Mesenchymal stromal/stem cells (MSCs) have demonstrated favorable wound healing properties *via* injury-activated trophic mechanisms and by generating an anti-inflammatory cytokine expression profile that alters fibroblast behavior to form a less dense, fibrotic granulation tissue (1–3). MSCs enable the healing of wounds that have inadequate microvasculature by expressing factors such as vascular endothelial growth factor-A to promote the proliferation of microvascular endothelial cells and subsequent angiogenesis that leads to nutrient delivery to fibroblasts and a long-lasting functional vascular network (4–8). MSCs promote keratinocyte proliferation and inhibition of myofibroblast differentiation, which attenuates the development of fibrotic scar tissue (9,10). In our previous work, MSCs encapsulated in a thiolated gelatin poly (ethylene glycol) (Gel-PEG-Cys) and poly (ethylene glycol)-diacrylate (PEGdA) crosslinked hydrogel demonstrated extensive cytoplasmic spreading, formation of cellular networks, improved cellular delivery, improved focal adhesion, and an immunophenotype change that led to the release of anti-inflammatory cytokines that accelerated wound healing and promoted cosmesis (11–13). In addition, MSC multipotency is maintained in the hydrogel environment and is enhanced in the presence of monocytes (12). This hydrogel system has also shown to release loaded solutes with controlled kinetics depending on gelatin and PEG composition. For example, hydrogels simultaneously loaded with silver sulfadiazine and bupivacaine achieved antimicrobial efficacy on *Staphylococcus aureus* (SA) and methicillin-resistant SA while promoting cutaneous wound healing (14–16).

The therapeutic potential of implanted MSC-loaded hydrogels could be limited by non-specific protein adsorption that facilitates the initial adhesion of native microorganisms

David Antonio Cantu contributed significantly to this work

Electronic supplementary material The online version of this article (doi:10.1208/s12248-015-9728-6) contains supplementary material, which is available to authorized users.

[1] School of Pharmacy, Division of Pharmaceutical Sciences, Pharmacy Practice Division, University of Wisconsin-Madison, 777 Highland Avenue, 7123 Rennebohm Hall, Madison, WI 53705, USA.
[2] Department of Biomedical Engineering, College of Engineering, University of Wisconsin-Madison, Madison, WI 53705, USA.
[3] Department of Medicine, School of Medicine and Public Health, University of Wisconsin-Madison, 1685 Highland Avenue, Madison, WI 53705, USA.
[4] Department of Surgery, School of Medicine and Public Health, University of Wisconsin-Madison, Madison, WI 53705, USA.
[5] University of Wisconsin Carbone Cancer Center, University of Wisconsin-Madison, Madison, WI 53705, USA.
[6] To whom correspondence should be addressed. (e-mail: WJKao@pharmacy.wisc.edu)

such as SA followed by continued growth and replication, extracellular polymer substance secretion (EPS), and eventual biofilm formation (17,18). Mature SA biofilm is highly resistant to immune cell recognition and elimination and bactericidal/bacteriostatic activity because of the presence of a thick EPS layer and metabolically senescent biofilm-associated bacteria (18). Biofilms can persist on implant surfaces before transitioning to a virulent state where bacteria secretes extracellular toxins and creates an acidic and hypoxic microenvironment that contributes to primary immune cell death, tissue necrosis, and device failure (19). Biofilm sloughing from the implant surface and dysfunctional innate immune responses lead to high secretion of proteases, reactive oxygen species (ROS), and pro-inflammatory cytokines at the implant site that contribute to patient comorbiditiy, aseptic loosening, and mortality (20,21). MSC administration was shown to promote host survival following cecal ligation, and puncture in rats have demonstrated attenuated monocyte/macrophage pro-inflammatory cytokine secretion, enhanced microbial pathogen elimination mediated by blood stream circulating neutrophils, attenuated neutrophil extravasation, and inhibited oxidative damage to multi-organ systems by preventing septic shock (22). However, the MSC-mediated impact on monocyte/macrophages or polymorphonuclear cells (PMNs) and gram-positive SA as multicellular biofilms or planktonic bacteria remains poorly understood. In this study, we investigate the ability of blood-derived leukocytes and hydrogel entrapped MSCs to abrogate SA colony-forming potential. We then develop minocycline and MSC-loaded hydrogels to investigate their potential in reducing SA colony-forming abilities. We hypothesized that blood-derived leukocytes and hydrogel entrapped MSCs cannot abrogate SA colony-forming potential but that minocycline and MSC-loaded hydrogels will reduce the colony-forming ability of planktonic SA while maintaining MSC metabolic viability and multipotency.

MATERIALS AND METHODS

Cell Isolation

Human Leukocyte and Autologous Serum Isolation. Venipuncture was executed on healthy, medication-refrained donors after obtaining written consent approved by the University of Wisconsin Hospital and Clinics Regulatory Committee. Monocytes and PMNs were isolated from whole blood using established density gradient methods (23). The collected monocytes were examined for purity using CD14-PE (AbD Serotec, Raleigh, NC) and CD45-FITC (BD Biosciences) monoclonal antibodies with appropriate fluorescence-minus-one and negative controls, which resulted in ~80–90% monocyte purity with the contaminant being lymphocytes using flow cytometry characterization (24,25). Autologous human serum (AHS) was obtained from whole blood without sodium citrate as previously described (23,26).

MSC Isolation, Characterization, and Encapsulation. MSCs were isolated from bone marrow aspirate filters harvested from healthy human donors following written consent approved by the University of Wisconsin Hospital and Clinics Regulatory Committee per our published protocols (12). Isolated MSCs (passage 4) were positive for MSC cell surface markers CD29-PE, CD44-PE, CD54-PE, CD73-PE, CD90-APC (BD Biosciences, San Jose, CA), and CD105-APC (eBiosciences Inc., San Diego, CA) and were negative for hematopoietic makers CD34-FITC, CD45-PE, CD31-PE (BD Biosciences) using monoclonal antibodies (with negative antibody gating controls) and analyzed using FACSCalibur flow cytometer with CellQuest acquisition software (BD Biosciences) and FlowJo software (Tree Star, Ashland, OR) (27,28). MSC multidifferentiation potential into osteoblasts, chondrocytes, and adipocytes was validated by culturing in Osteo NHdiff medium (10 days), Chondro NHdiff (14 days), and Adipo NHdiff medium (14 days) (BD Biosciences) in 48-well culture plates (Miltenyi Biotec, Auburn, CA) with successive medium changes every 4 days and differentiation detection following consensus MSC characterization criteria as stated previously (28). Only MSCs (passage 4–8) were used in this study. Gelatin + poly (ethylene) glycol (PEG) biomatricies were fabricated by adding Irgacure 2959 photoinitiator (0.5%, BASF, Ludwigshafen, Germany) to a sterile-filtered 20% (*w/v*) PEG-diacrylate (PEGdA) solution and a 20% (*w/v*) Gel-PEG-Cys solution. Gel-PEG-Cys was then mixed with PEGdA in respective ratios 1:1 ratio for 10% Gel-PEG-Cys + 10% PEGdA hydrogels and 5:3 for 12.5% Gel-PEG-Cys + 7.5% PEGdA hydrogels and MSC cell suspension to obtain a final concentration of 1×10^6 cells/mL. In hydrogels with minocycline (Research Products International Crop., Mt. Prospect, IL), both Gel-PEG-Cys and PEGdA solutions were made at 0.2 mg/mL before formulation. The polymer solution was pipetted into a glass-bottom Petri dish (*In Vitro* Scientific, Sunnyvale, CA) with a circular recess and then polymerized by exposing to UV light (λ_{max}=365 nm, 100 W/cm^2) for 2 min. MSC medium consisting of Dulbecco's Modified Eagle Medium (DMEM, Cellgro Mediatech, Inc.), 10% fetal bovine serum (FBS), 2 mM L-glutamine, and 2 mM non-essential amino acids (NEAA) was added to the tissue culture Petri dish, and the hydrogels were swollen for 24 h. For hydrogels containing minocycline, they were swollen in medium made at 0.2 mg/mL minocycline to ensure loading density. Collagen-only hydrogels were used for comparison to determine the impact of MSC-encapsulating material on MSC-leukocyte/SA interactions. Type I rat-tail collagen (2 mg/mL, BD Biosciences) was mixed with phosphate-buffered saline (PBS) (10×), DMEM, and 1 N NaOH (Sigma-Aldrich) to obtain a neutralized solution. The collagen solution was nucleated on ice for 35 min before adding a cell suspension to obtain a concentration of 1×10^6 MSCs/mL. The collagen solutions were pipetted into a tissue culture polystyrene (TCPS) plate (24-well plate, Costar®, Corning Inc., Corning, NY) and was incubated for 15 min (37°C) before MSC medium was added.

S. aureus Culture (Biofilm and Planktonic). SA (ATCC strain #29213, Manassas, VA) culture vials stored at −80°C were thawed and plated on trypticase soy agar (TSA, Becton Dickinson, Sparks, MD) Petri dishes (Fischer Scientific) that were then incubated for 24 h prior to biofilm or planktonic inoculation. For biofilm inoculation, SA colonies were removed and transferred to a tissue culture glass test tube containing ddH_2O, which was adjusted to match a 1.0 McFarland turbidity standard (3.0×10^8 CFU/mL) as measured by the densimeter (Grant Instruments, Cambridge, GB). The SA suspension was transferred to inoculate 22 mL of trypticase soy broth (TSB, Becton

Dickinson) growth media supplemented with 1% α-D-glucose (Sigma-Aldrich) at a 1:30 ratio of SA to TSB. Then 200 μL of TSB was added to each well of the 96 well plate MBEC™ HTP assay (Innovotech, Bozeman, MT) and placed on a rocking platform with 5 rocks per minute at 10° inclination for either 6 or 24 h incubation at 37°C to form nascent (6 h) or mature (24 h) biofilms on the 96-well plate TCPS pegs (29). For planktonic inoculation, SA colonies were removed and transferred to a tissue culture glass test tube containing ddH_2O, which was adjusted to match a 0.5 McFarland turbidity standard (1.5 x 10^8 CFU/mL) as measured by the densimeter. The SA suspension was transferred to inoculate 40 mL of TSB supplemented with 1% α-D-glucose (Sigma-Aldrich) at a 1:50 ratio of SA to TSB in a 50 mL conical tube. The SA culture was allowed to proliferate in suspension using a shaker plate rotating at 170 rpm that was incubated at 37°C for 5–6 h until the exponential (E1) growth phase optical density (OD_{600}=0.5, ~1×10^7 CFU/mL) was achieved as measured by the spectrophotometer (Nanodrop 2000x UV–vis Spectrophotometer, Thermo Scientific).

MSC + Leukocyte + SA Co-culture and Characterization

Co-culture Conditions. SA nascent (6 h) or established (24 h) biofilms on 96-well plate TCPS pegs were removed and directly placed in Roswell Park Memorial Institute medium (RPMI) 1640 supplemented with 10% AHS for 2, 6, or 12 h of transwell 24-well plate (Costar) co-culture at 37°C and 5% CO_2 incubation. Planktonic SA (OD_{600}=0.5, ~1×10^7 CFU/mL) was centrifuged at 5000*g* for 10 min and resuspended in RPMI 1640 supplemented with 1% AHS with or without PMNs (1×10^6 cells/mL) for 2 or 4 h of co-culture at 37°C and 5% CO_2 incubation. The hydrogel encapsulated MSC (MSC-Gel-PEG-Cys) or collagen-encapsulated MSC (MSC-collagen) concentration was maintained at 1×10^6 cells/mL and the monocyte or PMN concentration was maintained at 1×10^6 cells/mL (12). MSCs were cultured in the bottom chamber of the transwell (0.6 mL) and SA was cultured in the top chamber (0.2 mL) containing SA, SA, and monocyte, or SA and PMNs separated by a polycarbonate transwell insert (0.3 μm pore size). Minocycline (2 mg/mL) was utilized as a positive control. Specific conditions tested in co-culture for later viability and CFU/mL colony enumeration of SA (planktonic bacteria or biofilm) proceeds as follows: (1) SA-only; (2) SA + minocycline (2 mg/mL); (3) SA + MSC-Gel-PEG; (4) SA + MSC-collagen; (5) SA + monocyte or PMN + MSC-Gel-PEG; (6) SA + monocyte or PMN + MSC-collagen; and (7) SA + monocyte or PMN. For hydrogel growth inhibition of planktonic SA, hydrogels were placed directly in 0.8 mL of SA (OD_{600}=0.5, ~1×10^7 CFU/mL) in 24-well plates (Celltreat®, Shirley, MA) and co-cultures at 37°C (no humidity) for 16 h.

Viability Characterization and Log Colony-Forming Unit/mL Enumeration. After co-cultures, RPMI 1640 media supplemented with AHS was removed and the polycarbonate transwell surface (top chamber) with adherent monocytes or PMNs and encapsulated MSCs (bottom chamber) were washed with PBS (2×) and then incubated at 37°C with calcien AM/ethidium homodimer (4/2 μM, LIVE/DEAD®, Invitrogen) for 30 min. The transwell surface and the entrapped MSCs were then visualized for cell viability using an epifluorescent microscope (Olympus TE300, Center Valley, PA). MSCs and monocytes or PMNs in monoculture or co-culture without exposure to SA (planktonic or biofilm) was utilized as controls for comparison. After co-culture for the biofilm SA conditions, the TCPS pins were removed from co-culture and placed in 48-well plates (Costar) containing 200 μL of 0.9% NaCl, and were then sonicated (Fischer Scientific™ Mechanical Ultrasonic Cleaners) for 15 min to remove biofilm-associated SA (29). Then 100 μL of the SA was removed and serially diluted (1:10) in 1.5-mL Eppendorf tubes containing 0.9 mL of 0.9% NaCl. TSA Petri dishes were demarcated into four quadrants that were spotted three times for each quadrant with 20 μL of the SA suspension for each particular serial dilution. SA spots were allowed to dry for 30 min at room temperature to avoid dripping of the NaCl/SA solutions before incubating the TSA petri dishes at 37°C for 24 h in an inverted position. Viable colony enumeration was directly observed and Log colony-forming unit/mL (Log CFU/mL) was determined for each culture condition. After co-culture for the planktonic SA conditions, 0.25% of trypsin/EDTA (0.2 mL) was added to each well and incubated at 37°C for 5 min to remove any adsorbed PMNs or planktonic SA from the transwell culture wells. The entire culture volume was collected and centrifuged in 1.5-mL Eppendorf tubes at 5000*g* for 10 min to pellet SA and PMNs, then resuspended in 1 mL of PBS containing 0.1% saponin, which was allowed to incubate at 4°C for 20 min to induce PMN lysis (30). Each Eppendorf tube was again centrifuged at 5000*g* for 10 min, resuspended in 200 μL of 0.9% NaCl, serially diluted (1:10), spotted on TSA Petri dishes, and enumerated as described above.

Supernatant Analysis of Cytokine and PMN Granule Content Expression. Supernatant samples were also collected for the co-culture conditions: (1) SA + MSC-Gel-PEG; (2) SA + MSC-collagen; (3) SA + PMN + MSC-Gel-PEG; (4) SA + PMN + MSC-collagen; (5) SA + PMN with SA both in the biofilm or planktonic for 4 h of co-culture. Supernatant samples were centrifuged at 10,000g for 10 min and 50 μL of protein sample was subsequently analyzed by Bio-Plex protein detection and quantification (Bio-Rad, Hercules, CA) following the manufacturer's instructions for protein quantification of tumor necrosis factor-α (TNF-α), interleukin-6 (IL-6), myeloperoxidase (MPO) as a marker for primary PMN granules, and matrix metalloproteinase-9 (MMP-9) as a marker for tertiary PMN granules.

MSC + Minocycline-Loaded Hydrogel + SA co-Culture and Characterization

Toxicity of Endogenous Minocycline on MSCs. MSCs were plated at 40,000 cells/mL in 96-well TCPS plates (BD Biosciences) that had been pre-incubated with 0.1% gelatin solution for 24 h. A 10 mg/mL stock of minocycline in growth medium was made and appropriate amounts were added to each plate to make 0, 0.05, 0.1, 0.15, 0.2, and 0.5 mg/mL

minocycline treatment conditions and plates were incubated for 1, 3, 5, and 7 days. Respective media was changed after 3 days in the 5 and 7 day treatment groups to avoid cell death as a result of lack of nutrients in media and buildup of toxic metabolism by-products. After treatment times, media was removed from the well and the plate was incubated at 37°C with calcien AM/ethidium homodimer (4/2 μM, LIVE/DEAD®, Invitrogen) for 30 min. All wells were then imaged for viability using an epifluorescent microscope (Olympus TE300, Center Valley, PA) and then analyzed on a FLUOstar Omega platereader (BMG Labtech, Cary, NC) for necrotic cells ($\lambda_{excitation}$=544 nm, $\lambda_{emission}$=620 nm). LIVE/DEAD® was then removed from the well and a 1:10 CellTiter-Blue®: growth medium (Promega, Madison, WI) was added to each well and incubated at 37°C for 4 h. After incubation, plates were analyzed on a FLUOstar Omega platereader for metabolic activity ($\lambda_{excitation}$=544 nm, $\lambda_{emission}$=590 nm). MSCs (1×10^6 cells/mL) were also encapsulated in either 12.5% Gel-PEG-Cys or 10% Gel-PEG-Cys hydrogels as stated above, exposed to 0.2 mg/mL or 0 mg/mL minocycline, and swollen in respective media concentrations of minocycline for 24 h. Hydrogels were then transferred to 24-well plates (Celltreat®) and treated with LIVE/DEAD® and analyzed on an epifluorescent scope as stated above. LIVE/DEAD® was then removed and the hydrogels were analyzed for metabolic activity using a CellTiter-Blue® dilution as stated above.

Growth Inhibition of Planktonic SA with Hydrogels Loaded with MSCs and/or Minocycline. Hydrogels were made with encapsulated MSCs (1×10^6 cells/mL) with or without 0.2 mg/mL minocycline. All hydrogel conditions were made in triplicates with 12.5% Gel-PEG-Cys or 10% Gel-PEG-Cys and swollen for 24 h in respective minocycline concentration medium. Planktonic bacteria (OD_{600}=0.5, ~1×10^7 CFU/mL) was centrifuged at 5000*g* for 10 min and resuspended in MSC growth medium. Hydrogels were transferred to 24-well plates (Celltreat®) in a 800 μL planktonic SA solution in MSC growth medium. At 2, 4, and 16 h, 100 μL of the SA was removed and serially diluted (1:10) in 1.5-mL Eppendorf tubes containing 0.9 mL of 0.9% NaCl and TSA petri dishes were plated and analyzed for Log CFU/mL as stated above. Hydrogels were then removed from the SA culture and washed in a 24-well plate (Celltreat®) with PBS twice and transferred at another 24-well plate (Celltreat®) for LIVE/DEAD® analysis with subsequent imaging as stated above. Live and dead MSC cell counts were done using ImageJ software (National Institutes of Health, Bethesda, MD).

MSC Differentiation Detection. MSCs encapsulated in 10% Gel-PEG-Cys hydrogels with 0.2 mg/mL minocycline and swollen for 24 h with 0.2 mg/mL minocycline growth media were analyzed for differentiation potential to ensure MSC multipotency was maintained in the presence of minocycline. MSCs were either cultured in commercially available osteo NHdiff medium (10 days), chondro NHdiff medium (14 days), or adipo NHdiff medium (14 days) (BD Biosciences) with medium changes every 4 days. After differentiation, hydrogels were embedded in a 20% agarose (Invitrogen) and 1% formalin (Sigma-Aldrich) solution. Osteogenic and chondrogenic differentiated hydrogels were then placed in 70% ethanol overnight and then paraffin-embedded embedded and sectioned. Adpiogenic differentiated hydrogels were dehydrated in 20% sucrose (Sigma-Aldrich) after embedding for 1 day and then 1:1 20% sucrose: optimal cutting temperature (O.C.T.) for 1 day followed by placement in a cryomold in 100% O.C.T. and frozen on dry ice and cryosectioned. All images were taken at 200x on a Leica DM LB Microscope (Leica Microsystems, Wetzlar, Germany) unless otherwise stated. Osteogenic determination was performed with alizarin red S with Mayer's hematoxylin staining and with Von Kossa with nuclear fast red staining method to show calcium deposits seen in osteocytes (12,31,32). Chodrogenic determination was done with safranin O staining, which stains cartilaginous tissue, and immunostained with an aggrecan antibody, a proteoglycan highly expressed in cartilage tissue (12, 33, 34). The immunostained chodrogenic cells were imaged at 200x on a DSU Spinning Disk Confocal Microscope (Olympus, Center Valley, PA). Adipogenic determination was done with oil red O staining, which stains for triglycerides and lipid, and counterstained with Mayer's hematoxylin (12,35).

Statistical Analyses

All assays were tested in triplicates using independent replicates (n=3) with matched primary MSC (three separate donors), leukocyte (three separate donors), and hydrogels (three separately synthesized hydrogels). A two-way ANOVA for multiple comparisons was used to compare Log CFU/mL means among all co-culture conditions. An unpaired Student's t test was used to compare live cell percentage values between hydrogels with minocycline and hydrogels without minocycline after exposure to SA. A p value <0.05 was considered statistically significant (12).

RESULTS

SA Colony-Forming Capabilities in the Presence of Leukocytes and MSCs

Following 2 h of PMN + MSC co-culture in the presence of biofilm-associated SA, viability remained high for both PMNs and encapsulated MSCs in the presence of an established biofilm (Fig. 1) as well as in the presence of a nascent biofilm. Co-culture conditions (SA + MSC, SA + PMN + MSC, or SA + PMN) did not show a significant decrease in SA Log CFU/mL following 2 and 4 h of culture regardless of biofilm maturity as compared to the SA-only condition (Fig. 2). SA + minocycline was statistically lower than the SA-only Log CFU/mL value following 2 h of co-culture with an average Log CFU/mL that was similar regardless of biofilm maturity. In the presence of biofilm-associated SA, monocyte viability after 6 and 12 h of co-culture was substantially decreased for the SA + monocyte + MSC-Gel-PEG condition as compared to the SA + monocyte and SA + monocyte + MSC-collagen conditions (Supplementary Fig. 1). MSC viability remained high when encapsulated in both materials (Gel-PEG-Cys and collagen). In the co-

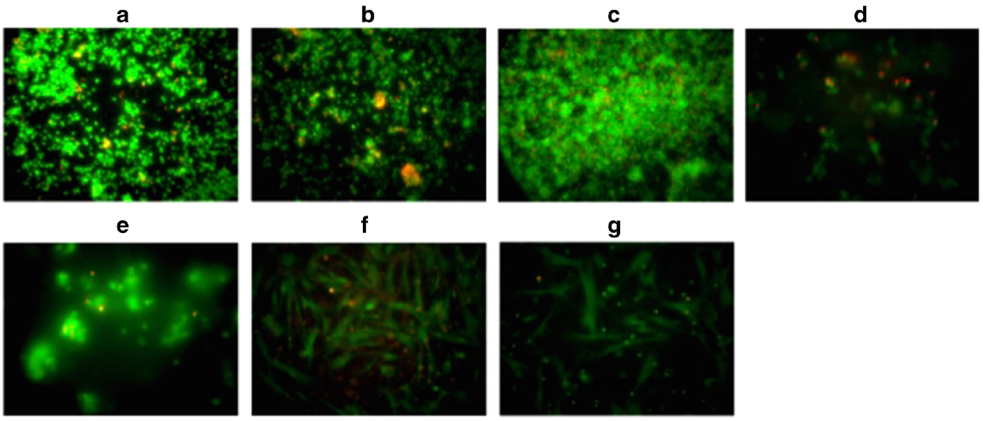

Fig. 1. PMN and MSC viability in the presence of 24 h established biofilm-associated SA after 2 h of co-culture at ×200 magnification. Adherent PMN viability in co-culture with **a** Gel-PEG-Cys-encapsulated MSCs and biofilm-associated SA, **b** biofilm-associated SA, and c collagen-encapsulated MSCs and biofilm-associated SA. Gel-PEG-Cys-encapsulated MSC viability in co-culture with **d** biofilm-associated SA and **e** adherent PMNs and biofilm-associated SA. Collagen-encapsulated MSC viability in co-culture with **f** biofilm-associated SA and **g** adherent PMNs and biofilm-associated SA

culture conditions with monocytes, no significant decrease in Log CFU/mL values at both 6 and 12 h was observed (Supplementary Fig. 2). SA + minocycline was statistically lower than the SA-only Log CFU/mL value for both 6 and 12 h of co-culture with similar average Log CFU/mL values.

In the presence of planktonic SA, PMN viability was significantly decreased both at 2 and 4 h for both SA + PMN and SA + PMN + MSC (Gel-PEG-Cys or collagen-encapsulated) conditions (Fig. 3). MSC viability remained high at 2 h when encapsulated in both materials in monoculture and co-culture with planktonic SA; however, by 4 h, the viability slightly decreased for Gel-PEG-Cys encapsulated MSCs as compared to collagen encapsulated MSCs. After 2 and 4 h of co-culture, there was no observed statistical difference in Log CFU/mL between SA-only and SA co-culture conditions (Fig. 4). SA + minocycline was statistically lower than the SA-only Log CFU/mL value for both time points with an average Log CFU/mL value that was lower at 4 h exposure as compared to 2 h, which was not observed in biofilm-associated SA co-culture experiments. Planktonic SA demonstrated higher Log CFU/mL than in biofilm-associated SA alone and in all co-cultures.

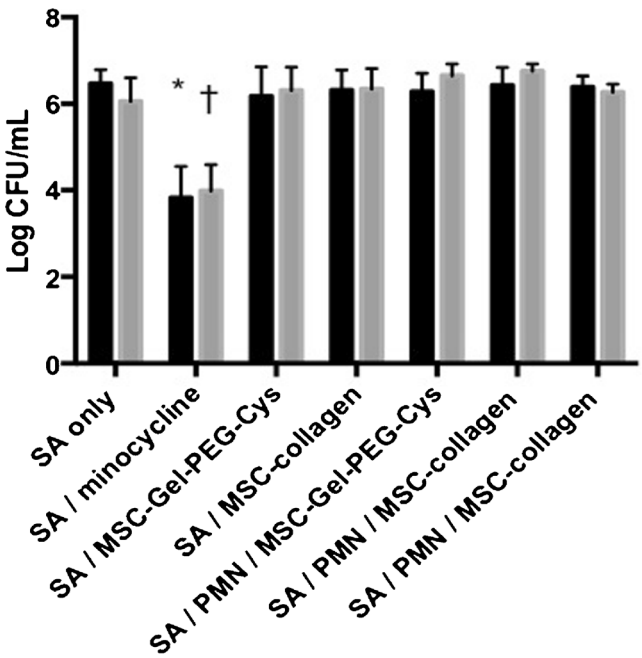

Fig. 2. Biofilm-associated SA Log CFU/mL for 6 h (■) and 24 h (■) of biofilm growth after 2 h MSC-PMN co-culture. $P<0.05$ *versus* SA-only condition for 6 h nascent biofilm (*asterisk*) and for 24 h mature biofilm (*dagger*) after 2 h of co-culture

TNF-α, IL-6, MPO, and MMP-9 were assayed to gain insight into the induction or attenuation of PMN inflammatory response in the presence of SA (Supplementary Fig. 3). TNF-α concentrations were extremely low for all conditions when compared with observed normal (10–17 pg/mL) and elevated (23–32 pg/mL) levels in human serum (36,37). IL-6 concentrations were detectable in all MSC co-culture conditions and undetectable in the SA + PMN co-culture. All detectable IL-6 concentrations were higher than observed normal (10–65 pg/mL) and elevated (30–80 pg/mL) levels in human serum (37,38). MPO was detectable in all MSC co-culture conditions, demonstrating higher than normal MPO levels in healthy human serum (37–46 ng/mL) (39). MPO levels were attenuated in the SA + PMN + MSC-collagen and SA + PMN co-culture conditions. As a biomarker for PMN tertiary granule release, MMP-9 was detectable in all co-culture conditions with PMNs but undetectable in the SA + MSC conditions. MMP-9 levels in PMN co-cultures were around observed normal (30–50 ng/mL) human serum levels and lower than observed elevated (200–500 ng/mL) human serum levels (40). Taken together, PMN innate immunity activation was attenuated as a result of co-culture with SA.

MSC Viability in Hydrogels Loaded With Minocycline

To determine hydrogel loading concentrations of minocycline to prevent SA growth and maintain metabolically viable MSCs, exogenous dosing of minocycline on MSCs was done. The 0.05–0.2 mg/mL minocycline conditions showed comparable MSC viability as no minocycline after 1, 3, 5, and 7 days exposure (Supplementary Fig. 4). MSC

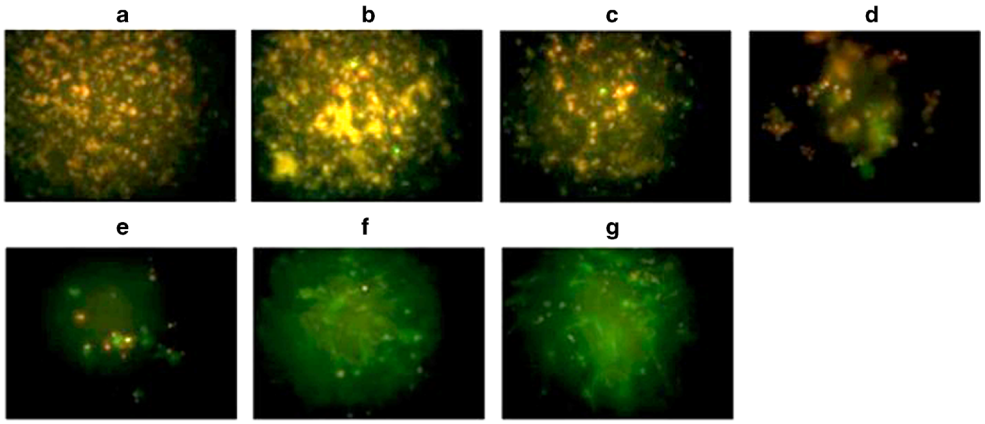

Fig. 3. PMN and MSC viability in the presence of planktonic SA (OD_{600}=0.5) after 4 h of co-culture at ×200 magnification. Adherent PMN viability in co-culture with **a** Gel-PEG-Cys-encapsulated MSCs and planktonic SA, **b** planktonic SA, and **c** collagen-encapsulated MSCs and planktonic SA. Gel-PEG-Cys-encapsulated MSC viability in co-culture with **d** planktonic SA and **e** polycarbonate-adherent PMNs and planktonic SA. Collagen-encapsulated MSC viability in co-culture with **f** adherent PMNs and planktonic SA and **g** adherent PMNs and planktonic SA

viability was significantly decreased at 0.5 mg/mL minocycline. Mean fluorescent intensities (MFI) for necrotic MSCs were significantly higher in the 0.2 and 0.5 mg/mL minocycline conditions after 1, 3, and 5 day exposure compared to MSCs with no minocycline (Table I). Necrotic MSC MFI was significantly higher only in the 0.5 mg/mL minocycline condition after 7 day exposure. MFI for metabolic activity was significantly lower in the 0.5 mg/mL minocycline condition after 1, 3, 5, and 7 day exposure compared to MSCs with no minocycline. Therefore, 0.2 mg/mL minocycline was utilized as the loading concentration of minocycline within hydrogels entrapped with MSCs.

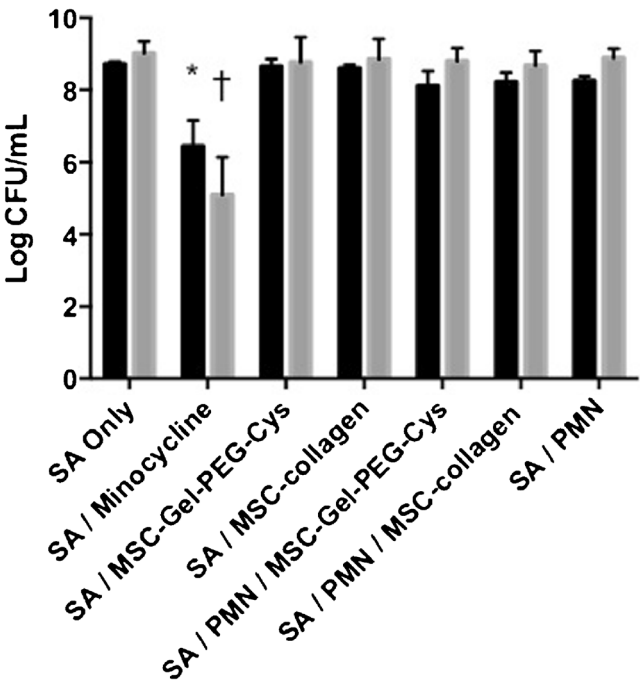

Fig. 4. Planktonic (OD_{600}=0.5) SA Log CFU/mL after 2 h (■) and 4 h (▒) MSC-PMN co-culture. $P<0.05$ *versus* SA-only condition for 2 h co-culture (*asterisk*) and 4 h co-culture (*dagger*)

To determine target Gel-PEG-Cys concentration for optimal MSC metabolic activity in hydrogels, metabolic activity of hydrogel-entrained MSCs was measured in 10, 7.5, and 5% wt/vol.% Gel-PEG-Cys. Ten percent Gel-PEG-Cys hydrogels showed a MFI of 17.2±0.9, 7.5% Gel-PEG-Cys hydrogels showed a MFI of 14.2±0.5, and 5% Gel-PEG-Cys hydrogels showed a MFI of 9.3±0.1 with 10% Gel-PEG-Cys demonstrating significantly higher MFI values than 7.5 and 5% Gel-PEG-Cys hydrogels. For subsequent study, 12.5 and 10% Gel-PEG-Cys hydrogels were selected. MSC metabolic activity from cell titer blue MFI was normalized by comparing results to cell titer blue MFI in hydrogels with no MSC encapsulation. Metabolic activity of MSCs in 12.5 and 10% Gel-PEG-Cys hydrogels with or without entrapped minocycline (0.2 mg/mL) showed no significant differences (Fig. 5). These results suggest that MSCs are as metabolically active in hydrogels after the 24 h in 0.2 mg/mL minocycline.

SA Growth Inhibition by Hydrogels Loaded With MSC + Minocycline

After 2, 4, and 16 h of co-culture, SA Log CFU/mL was significantly lowered in the presence of hydrogels loaded with minocycline with and without entrapped MSCs (Fig. 6), both in 12.5 and 10% Gel-PEG-Cys hydrogels. MSCs in 12.5 or 10% Gel-PEG-Cys hydrogels in co-culture with SA showed significantly lower live/dead cell ratios compared to respective hydrogels with 0.2 mg/mL minocycline, suggesting the addition of minocycline to hydrogels maintains MSC viability in the presence of SA (Fig. 7). MSCs loaded at 0.2 mg/mL minocycline demonstrated multipotency with ability to differentiate into osteogenic, chondrogenic, and adipogenic cells (Fig. 8). Osteogenic MSCs stained positively both with Alizarin Red S (counterstained with Mayer's Hematoxylin) and with the Von Kossa method (counterstained with Nuclear Fast Red) after 10 days of hydrogel culture in osteogenic differentiation medium. Chondrogenic MSCs stained positively both for Safranin O (counterstained with FCF Green) and with an aggrecan antibody (tagged with a secondary antibody conjugated to Alexa Fluor 555 and counterstained

Table I. Mean Fluorescent Intensity (MFI) Values (x10,000) for Necrotic Cells (Top Value, at 620 nm) and Metabolic Activity (Lower Value, at 590 nm) of MSCs After Exposure to Minocycline Doses Through 7 Days

MFI 620 nm				
MFI 590 nm	1 day	3 day	5 day	7 day
0 mg/mL	16.2±0.3	16.2±0.6	15.8±0.3	15.6±0.3
	13.5±0.4	13.6±0.8	12.8±1.3	13.2±1.2
0.05 mg/mL	16.4±0.4	16.3±0.6	15.8±0.4	15.6±0.4
	12.8±0.6	15.0±1.1	11.3±0.8	12.8±1.0
0.1 mg/mL	16.3±0.4	16.3±0.8	16.0±0.4	15.5±0.2
	12.8±0.4	15.1±0.9	11.5±0.2	11.9±0.4
0.15 mg/mL	16.7±0.3	16.3±0.8	16.0±0.4	15.5±0.5
	12.8±0.4	15.1±0.9	11.5±0.2	11.9±0.4
0.2 mg/mL	17.3±0.6*	16.8±0.8*	16.5±0.4*	16.1±0.1
	13.5±0.8	16.7±0.7	12 1±0.9	12.3±1.6
0.5 mg/mL	18.9±0.2*	18.8±0.2*	18.9±0.3*	18.9±0.3*
	10.9±0.4†	10.4±1.0†	5.6±0.9†	5.0±0.2†

*$P<0.05$ *versus* 0 mg/mL condition for MFI values for significantly higher necrotic cells; †$P<0.05$ *versus* 0 mg/mL condition for MFI values for significantly lower metabolic activity

with 4′,6-diamidino-2-phenylindole) after 14 days of hydrogel culture in chondrogenic differentiation medium. Adipogenic MSCs stained positively for Oil Red O (counterstained with Mayer's Hematoxylin) after 14 days of hydrogel culture in adipogenic differentiation medium.

DISCUSSION

SA abrogates primary blood-derived leukocyte bactericidal/bacteriostatic activity possibly by secreting Panton-Valentine leukocidin or γ-haemolysin and other virulence factors (41–43). Ineffective clearance of apoptotic PMNs can contribute to secondary necrosis and extensive tissue inflammation (43). PMN phagocytosis of SA induces a global gene expression differentiation program that accelerates PMN apoptosis by promoting pro-apoptotic factor up-regulation and down-regulation of innate immune cell receptor, anti-apoptotic factor, and pro-inflammatory cytokine expression (44,45). Microarray studies have shown that biofilm-associated SA up-regulate expression of formate dehydrogenase, arginine deiminase, and urease activity in increasingly anoxic and low pH conditions contributed by the production of metabolic by-products. Biofilm-associated SA also up-regulates several anti-oxidant factors such as

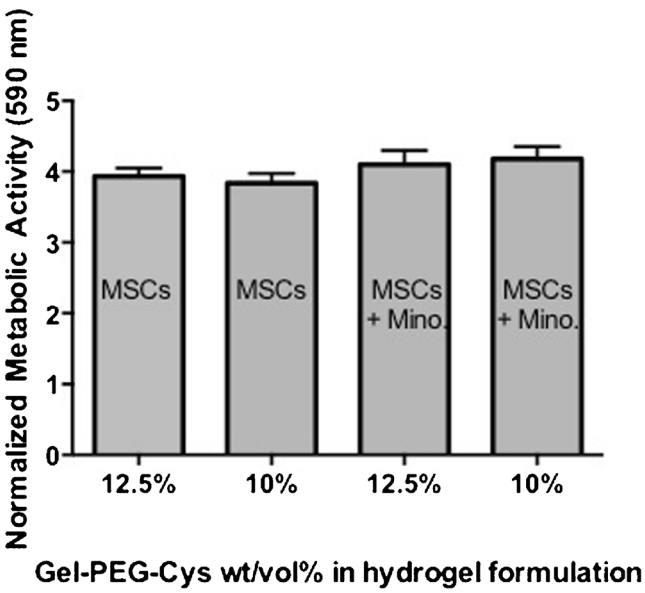

Fig. 5. Metabolic activity (MFI 590 nm) of MSCs in 1×10^6 cells/mL loaded hydrogels after 24 h of swelling at 12.5% Gel-PEG-Cys and 10% Gel-PEG-Cys in minocycline absent hydrogels and 0.2 mg/mL minocycline-loaded hydrogels compared to hydrogels with no MSCs. No significant differences between MSC metabolic activity in minocycline absent and minocycline-loaded hydrogels were observed

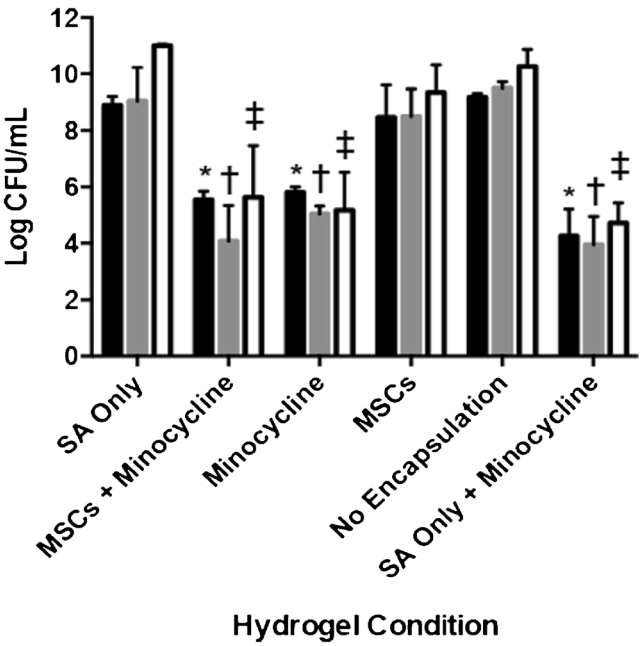

Fig. 6. Planktonic (OD_{600}=0.5) SA Log CFU/mL after 2 (■), 4 (▒), and 16 (□) h co-culture with hydrogels. Minocycline in 10% wt/vol.% Gel-PEG-Cys hydrogels indicate hydrogels made and swollen at 0.2 mg/mL minocycline and MSCs in hydrogels are at 1×10^6 cells/mL. Minocycline in SA-only + minocycline condition indicates SA suspension in 0.2 mg/mL minocycline. $P<0.05$ *versus* SA-only condition for 2 h (*asterisk*), 4 h (*dagger*), and 16 h (*double dagger*) co-culture

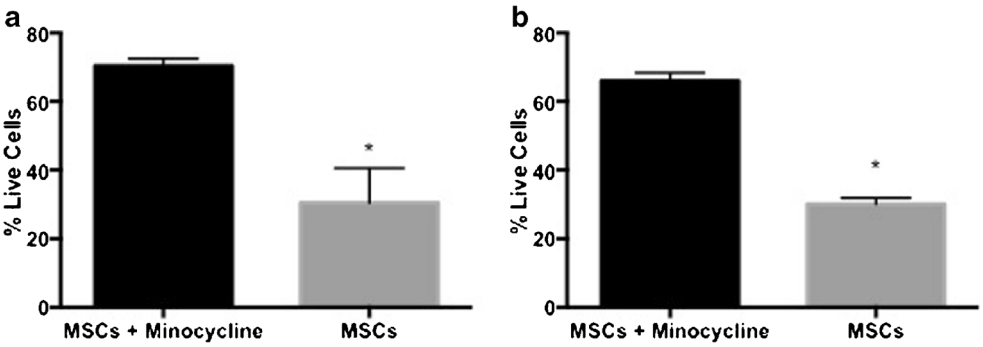

Fig. 7. Live/dead ratios of MSCs in hydrogels after 16 h co-culture with planktonic SA (OD_{600}=0.5) in 12.5% wt/vol.% Gel-PEG-Cys hydrogels (**a**) and 10% wt/vol.% Gel-PEG-Cys hydrogels (**b**). $P<0.05$ *versus* MSCs+minocycline condition (*asterisk*)

superoxide dismutase, staphyloxanthin, and glutathione peroxidase to mitigate oxidative damage and to resist the oxidative-mediated bactericidal activity of infiltrating leukocytes (46). Ineffectual biofilm-associated SA clearance could be contributed by poor opsonization, large size, physical complexity, and presence of the thick EPS later. The thick EPS later also limits SA ligand accessibility deterring patter recognition receptor (PRR) activation in leukocytes that would contribute to the elimination of SA within the bulk of the biofilm (47). There is a clear need for antibiotics to prevent SA biofilm formation from planktonic SA.

We observed a decrease in TNF-α by 4 h with planktonic SA suggesting loss of PMN function indicative of an extensive cell death observed at 4 h of planktonic SA co-culture. Although TNF-α is a critical pro-inflammatory cytokine necessary for resolving SA induced infection by infiltrating PMNs and monocyte/macrophages, TNF-α signaling demonstrates concentration-dependent effects on PMNs that can either extend neutrophil lifetime *via* an NF-κB mechanism or accelerate PMN cell death *via* caspase-dependent or ROS-dependent mechanisms (48,49). Greater IL-6 secretion from MSCs (paracrine) co-culture conditions may indicate a high viability of MSCs; however, the undetectable IL-6 secretion

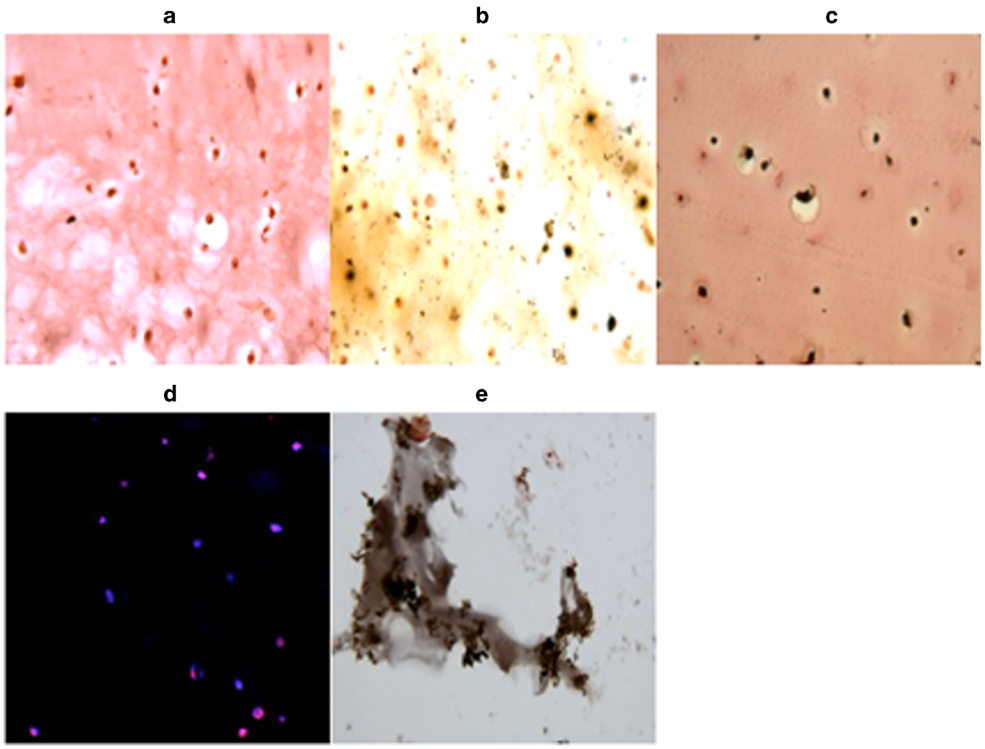

Fig. 8. MSC differentiation after 24 h of culture in 10% Gel-PEG-Cys wt/vol.% hydrogels swollen at 0.2 mg/mL minocycline at ×200 magnification. Osteogenic differntiation detected by **a** Alizarin Red S staining and counterstaining with Mayer's Hematoxylin; **b** Von Kossa staining and counterstaining with Nuclear Fast Red. Chondrogenic differentiation detected by **c** Safranin O staining and counterstaining with FCF Green; **d** aggrecan immunostaining (Alexa Fluor 555) and counterstaining with 4′,6-diamidino-2-phenylindole. Adpiogenic differentiation detected by **e** Oil Red O staining and counterstaining with Mayer's Hematoxylin

from PMN + SA co-culture suggests that IL-6 secretion is attenuated in PMNs, and extensive cell death of PMNs was observed in planktonic bacteria. IL-6 signaling from MSCs has been shown to delay spontaneous apoptosis of PMNs in extended co-culture and may have extended PMN viability (50). MPO expression was higher in MSC containing conditions compared to PMN containing conditions, which displayed normal MPO expression. MPO signaling can extend the survival of PMNs and prolong inflammation for the elimination of bacterial pathogens, and MSCs may express MPO that can extend PMN viability (51). The attenuated MPO signaling in PMNs demonstrates a disruption of PMN-mediated effector functions correlated with high bacterial Log CFU/mL concentrations and extensive cell death at 4 h co-culture. MMP-9 signaling at 4 h for planktonic SA co-culture was at normal levels in PMN containing conditions indicating the presence of MSCs or planktonic SA did not interfere with PMN chemotaxis or tertiary degranulation normally required for elimination for pathogenic microbes; however, MMP-9 signaling from PMNs may have also contributed to extensive PMN death *via* a caspase-dependent mechanism (52). Planktonic and biofilm-associated SA largely evaded the immunomodulatory activity of MSCs that had previously been shown to protect against septic shock and enhance leukocyte bacteriostatic/bactericidal activity in gram-negative septic of cecal ligation and puncture (CLP) animal models (53–55). However, MSC viability remained high for all culture conditions and did not appear sensitive to SA exotoxins or nucleases as the leukocytes did, possibly due to protection mediated by biomatrix encapsulation.

Minocycline is a second-generation tetracycline bacteriostatic prokaryotic protein synthesis inhibitor that has demonstrated strong biofilm-associated and planktonic growth inhibition of SA and has demonstrated effective infection elimination in uncomplicated skin and soft-tissue abscesses caused by methicillin-resistant SA while providing cytoprotective properties to eukaryotic cells (56–59). Minocycline has shown to inhibit the growth of SA alone while potentiating the effects of other antimicrobial agents by interrupting the cellular calcium balance in microbes (57). Minocycline is a highly lipophilic molecule and composite hydrogels have demonstrated efficient loading and zero-order release of hydrophobic drugs without precipitations, making Gel-PEG-Cys/PEGdA composite hydrogels a favorable drug delivery vehicle for minocycline (60,61). Minocycline inhibition of protein synthesis and attenuation of calcium homeostasis of SA may have prevented production and secretion of PVL or γ-haemolysin increasing MSC viability in minocycline-loaded hydrogels (57,41–43). Cytoprotective properties of minocycline may have also enhanced MSC viability in hydrogels loaded with minocycline and MSCs compared to hydrogels loaded with MSCs alone (62). Planktonic SA colony-forming abilities are inhibited while MSC viability and differentiation capacity were maintained in MSC and minocycline-loaded hydrogels. Our results suggest that minocycline can be loaded into MSC encapsulated hydrogels as a prophylactic measure against SA growth. Growth inhibition of planktonic SA through hydrogel minocycline release may prevent the formation of biofilm and subsequent systemic infection and may accelerate the wound healing properties of MSCs if the minocycline and MSC-loaded hydrogels were applied to wounds compared to hydrogels loaded only with MSCs and not with minocycline (18).

CONCLUSIONS

SA abrogates primary blood-derived leukocyte bactericidal/bacteriostatic activity alone and in the presence of encapsulated MSCs. MSCs were metabolically viable in Gel-PEG-Cys/PEGdA composite hydrogels loaded with minocycline at 0.2 mg/mL. Hydrogels loaded with MSCs and minocycline significantly inhibited planktonic SA colony-forming abilities while maintaining MSC viability, metabolic activity, and multipotency differentiation capacity.

ACKNOWLEDGMENTS

The authors would like to thank the University of Wisconsin Carbone Cancer Center Experimental Pathology Laboratory for their assistance in MSC histology. This research was supported in part by the University of Wisconsin-Madison School of Pharmacy, the National Institutes of Health HL115482 grant, the National Institutes of Health Biotechnology Training Program HL115482 grant, and the University of Wisconsin Science and Medicine Graduate Research Scholars Fellowship.

Conflict of Interest The authors indicate no potential conflicts of interest.

REFERENCES

1. Caplan AI. Why are MSCs therapeutic? New data: new insight. J Pathol. 2009;217(2):318–24.
2. Reitamo S, Remitz A, Tamai K, Uitto J. Interleukin-10 modulates type I collagen and matrix metalloprotease gene expression in cultured human skin fibroblasts. J Clin Invest. 1994;94(6):2489–92.
3. Jeon YK, Jang YH, Yoo DR, Kim SN, Lee SK, Nam MJ. Mesenchymal stem cells' interaction with skin: wound-healing effect on fibroblast cells and skin tissue. Wound Repair Regen. 2010;18(6):655–61.
4. Brown JM, Nemeth K, Kushnir-Sukhov NM, Metcalfe DD, Mezey E. Bone marrow stromal cells inhibit mast cell function *via* a COX2-dependent mechanism. Clin Exp Allergy. 2011;41(4):526–34.
5. Renault MA, Roncalli J, Tongers J, Misener S, Thorne T, Jujo K, *et al.* The Hedgehog transcription factor Gli3 modulates angiogenesis. Circ Res. 2009;105(8):818–26.
6. Gruber R, Kandler B, Holzmann P, Vögele-Kadletz M, Losert U, Fischer MB, *et al.* Bone marrow stromal cells can provide a local environment that favors migration and formation of tubular structures of endothelial cells. Tissue Eng. 2005;11(5–6):896–903.
7. Kaigler D, Krebsbach PH, Polverini PJ, Mooney DJ. Role of vascular endothelial growth factor in bone marrow stromal cell modulation of endothelial cells. Tissue Eng. 2003;9(1):95–103.
8. Au P, Tam J, Fukumura D, Jain RK. Bone marrow-derived mesenchymal stem cells facilitate engineering of long-lasting functional vasculature. Blood. 2008;111(9):4551–8.
9. Bevan D, Gherardi E, Fan TP, Edwards D, Warn R. Diverse and potent activities of HGF/SF in skin wound repair. J Pathol. 2004;203(3):831–8.

10. Shukla MN, Rose JL, Ray R, Lathrop KL, Ray A, Ray P. Hepatocyte growth factor inhibits epithelial to myofibroblast transition in lung cells *via* Smad7. Am J Respir Cell Mol Biol. 2009;40(6):643–53.
11. Fu Y, Xu K, Zheng X, Giacomin AJ, Mix AW, Kao WJ. 3D cell entrapment in crosslinked thiolated gelatin-poly (ethylene glycol) diacrylate hydrogels. Biomaterials. 2012;33(1):48–58.
12. Cantu DA, Hematti P, Kao WJ. Cell encapsulating biomaterial regulates mesenchymal stromal/stem cell differentiation and macrophage immunophenotype. Stem Cells Transl Med. 2012;1(10):740–9.
13. Wang C, Varshney RR, Wang DA. Therapeutic cell delivery and fate control in hydrogels and hydrogel hybrids. Adv Drug Deliv Rev. 2010;62(7–8):699–710.
14. Waldeck H, Kao WJ. Effect of the Addition of a Labile Gelatin Component on the Degradation and Solute Release Kinetics of a Stable PEG Hydrogel. J Biomater Sci Polym Ed. 2011.
15. Kleinbeck KR, Bader RA, Kao WJ. Concurrent *in vitro* release of silver sulfadiazine and bupivacaine from semi-interpenetrating networks for wound management. J Burn Care Res. 2009;30(1):98–104.
16. Fu Y, Kao WJ. Drug release kinetics and transport mechanisms of non-degradable and degradable polymeric delivery systems. Expert Opin Drug Deliv. 2010;7(4):429–44.
17. Busscher HJ, van der Mei HC, Subbiahdoss G, Jutte PC, van den Dungen JJ, Zaat SA, *et al.* Biomaterial-associated infection: locating the finish line in the race for the surface. Sci Transl Med. 2012;4 (153):153rv10.
18. Simoes M, Simoes LC, Vieira MJ. A review of current and emergent biofilm control strategies. Food Sci Technol. 2010;43:573–83.
19. Franz S, Rammelt S, Scharnweber D, Simon JC. Immune responses to implants—a review of the implications for the design of immunomodulatory biomaterials. Biomaterials. 2011;32(28):6692–709.
20. Arciola CR, Campoccia D, Speziale P, Montanaro L, Costerton JW. Biofilm formation in staphylococcus implant infections. A review of molecular mechanisms and implications for biofilm-resistant materials. Biomaterials. 2012;33(26):5967–82.
21. Fehring TK, Odum SM, Berend KR, Jiranek WA, Parvizi J, Bozic KJ, *et al.* Failure of irrigation and débridement for early postoperative periprosthetic infection. Clin Orthop Relat Res. 2013;471(1):250–7.
22. Tyndall A, Pistoia V. Mesenchymal stem cells combat sepsis. Nat Med. 2009;15(1):18–20.
23. Waldeck H, Wang X, Joyce E, Kao WJ. Active leukocyte detachment and apoptosis/necrosis on PEG hydrogels and the implication in the host inflammatory response. Biomaterials. 2012;33(1):29–37.
24. Maecker HT, Trotter J. Flow cytometry controls, instrument setup, and the determination of positivity. Cytometry A. 2006;69(9):1037–42.
25. Cohen HC, Joyce EJ, Kao WJ. Biomaterials selectively modulate interactions between human blood-derived polymorphonuclear leukocytes and monocytes. Am J Pathol. 2013;182(6):2180–90.
26. Wang X, Schmidt DR, Joyce EJ, Kao WJ. Application of MS-based proteomics to study serum protein adsorption/absorption and complement C3 activation on poly (ethylene glycol) hydrogels. J Biomater Sci Polym Ed. 2010.
27. Trivedi P, Hematti P. Derivation and immunological characterization of mesenchymal stromal cells from human embryonic stem cells. Exp Hematol. 2008;36(3):350–9.
28. Dominici M, Le Blanc K, Mueller I, Slaper-Cortenbach I, Marini F, Krause D, *et al.* Minimal criteria for defining multipotent mesenchymal stromal cells. Int Sociol Cell Ther position statement Cyt. 2006;8(4):315–7.
29. Ceri H, Olson ME, Stremick C, Read RR, Morck D, Buret A. The Calgary biofilm device: new technology for rapid determination of antibiotic susceptibilities of bacterial biofilms. J Clin Microbiol. 1999;37(6):1771–6.
30. Voyich JM, Braughton KR, Sturdevant DE, Whitney AR, Saïd-Salim B, Porcella SF, *et al.* Insights into mechanisms used by Staphylococcus aureus to avoid destruction by human neutrophils. J Immunol. 2005;175(6):3907–19.
31. Golic I, Velickovic K, Markelic M, Stancic A, Jankovic A, Vucetic M, *et al.* Calcium-induced alteration of mitochondrial morphology and mitochondrial-endoplasmic reticulum contacts in rat brown adipocytes. Eur J Histochem. 2014;58(3):2377.
32. Subbiah R, Du P, Van SY, Suhaeri M, Hwang MP, Lee K, *et al.* Fibronectin-tethered graphene oxide as an artificial matrix for osteogenesis. Biomed Mater. 2014;9(6):065003.
33. Pester JK, Stumpfe ST, Steinert S, Marintschev I, Plettenberg HK, Aurich M, *et al.* Histological, biochemical and spectroscopic changes of articular cartilage in osteoarthritis: is there a chance for spectroscopic evaluation? Z Orthop Unfall. 2014;152(5):469–79.
34. Yang M, Zhang L, Stevens J, Gibson G. CRISPR/Cas9 mediated generation of stable chondrocyte cell lines with targeted gene knockouts; analysis of an aggrecan knockout cell line. Bone. 2014;69C:118–25.
35. Li G, Yao W, Jiang H. Short-chain fatty acids enhance adipocyte differentiation in the stromal vascular fraction of porcine adipose tissue. J Nutr. 2014.
36. Aziz N, Nishanian P, Fahey JL. Levels of cytokines and immune activation markers in plasma in human immunodeficiency virus infection: quality control procedures. Clin Diagn Lab Immunol. 1998;5(6):755–61.
37. Lee SJ, Li Z, Sherman B, Foster CS. Serum levels of tumor necrosis factor-alpha and interleukin-6 in ocular cicatricial pemphigoid. Invest Optha & Vis Sci. 1993;34(13):3522–5.
38. Kleiner G, Marcuzzi A, Zanin V, Monasta L, Zauli G. Cytokine levels in the serum of healthy subjects. Mediators Inflamm. 2013;2013:434010.
39. Hoy A, Trégouët D, Leininger-Muller B, Poirier O, Maurice M, Sass C, *et al.* Serum myeloperoxidase concentration in a healthy population: biological variations, familial resemblance and new genetic polymorphisms. Eur J Hum Genet. 2001;9(10):780–6.
40. Chang YH, Lin IL, Tsay GJ, Yang SC, Yang TP, Ho KT, *et al.* Elevated circulatory MMP-2 and MMP-9 levels and activities in patients with rheumatoid arthritis and systemic lupus erythematosus. Clin Biochem. 2008;41(12):955–9.
41. Kobayashi SD, Braughton KR, Palazzolo-Ballance AM, Kennedy AD, Sampaio E, Kristosturyan E, *et al.* Rapid neutrophil destruction following phagocytosis of Staphylococcus aureus. J Innate Immun. 2010;2(6):560–75.
42. Bantel H, Sinha B, Domschke W, Peters G, Schulze-Osthoff K, Jänicke RU. Alpha-toxin is a mediator of staphylococcus aureus-induced cell death and activates caspases *via* the intrinsic death pathway independently of death receptor signaling. J Cell Biol. 2001;155(4):637–48.
43. Genestier AL, Michallet MC, Prévost G, Bellot G, Chalabreysse L, Peyrol S, *et al.* Staphylococcus aureus Panton-valentine leukocidin directly targets mitochondria and induces Bax-independent apoptosis of human neutrophils. J Clin Invest. 2005;115(11):3117–27.
44. Kobayashi SD, Braughton KR, Whitney AR, Voyich JM, Schwan TG, Musser JM, *et al.* Bacterial pathogens modulate an apoptosis differentiation program in human neutrophils. Proc Natl Acad Sci U S A. 2003;100(19):10948–53.
45. Kobayashi SD, Voyich JM, Buhl CL, Stahl RM, DeLeo FR. Global changes in gene expression by human polymorphonuclear leukocytes during receptor-mediated phagocytosis: cell fate is regulated at the level of gene expression. Proc Natl Acad Sci U S A. 2002;99(10):6901–6.
46. Resch A, Rosenstein R, Nerz C, Götz F. Differential gene expression profiling of Staphylococcus aureus cultivated under biofilm and planktonic conditions. Appl Environ Microbiol. 2005;71(5):2663–76.
47. Leid JG, Shirtliff ME, Costerton JW, Stoodley P. Human leukocytes adhere to, penetrate, and respond to Staphylococcus aureus biofilms. Infect Immun. 2002;70(11):6339–45.
48. Cowburn AS, Deighton J, Walmsley SR, Chilvers ER. The survival effect of TNF-alpha in human neutrophils is mediated *via* NF-kappa B-dependent IL-8 release. Eur J Immunol. 2004;34(6):1733–43.
49. Maianski NA, Roos D, Kuijpers TW. Tumor necrosis factor alpha induces a caspase-independent death pathway in human neutrophils. Blood. 2003;101(5):1987–95.

50. Raffaghello L, Bianchi G, Bertolotto M, Montecucco F, Busca A, Dallegri F, *et al*. Human mesenchymal stem cells inhibit neutrophil apoptosis: a model for neutrophil preservation in the bone marrow niche. Stem Cells. 2008;26(1):151–62.
51. El Kebir D, József L, Pan W, Filep JG. Myeloperoxidase delays neutrophil apoptosis through CD11b/CD18 integrins and prolongs inflammation. Circ Res. 2008;103(4):352–9.
52. Kolaczkowska E, Koziol A, Plytycz B, Arnold B, Opdenakker G. Altered apoptosis of inflammatory neutrophils in MMP-9-deficient mice is due to lower expression and activity of caspase-3. Immunol Lett. 2009;126(1–2):73–82.
53. Németh K, Leelahavanichkul A, Yuen PS, Mayer B, Parmelee A, Doi K, *et al*. Bone marrow stromal cells attenuate sepsis *via* prostaglandin E (2)-dependent reprogramming of host macrophages to increase their interleukin-10 production. Nat Med. 2009;15(1):42–9.
54. Choi H, Lee RH, Bazhanov N, Oh JY, Prockop DJ. Anti-inflammatory protein TSG-6 secreted by activated MSCs attenuates zymosan-induced mouse peritonitis by decreasing TLR2/NF-κB signaling in resident macrophages. Blood. 2011;118(2):330–8.
55. Mei SH, Haitsma JJ, Dos Santos CC, Deng Y, Lai PF, Slutsky AS, *et al*. Mesenchymal stem cells reduce inflammation while enhancing bacterial clearance and improving survival in sepsis. Am J Respir Crit Care Med. 2010;182(8):1047–57.
56. Schönfeld P, Siemen D, Kreutzmann P, Franz C, Wojtczak L. Interaction of the antibiotic minocycline with liver mitochondria—role of membrane permeabilization in the impairment of respiration. FEBS J. 2013;280(24):6589–99.
57. Li H, Zhang C, Liu P, Liu W, Gao Y, Sun S. *In vitro* interactions between fluconazole and minocycline against mixed cultures of Candida albicans and Staphylococcus aureus. J Microbiol Immunol Infect. 2014.
58. Cunha BA. Minocycline, often forgotten but preferred to trimethoprim-sulfamethoxazole or doxycycline for the treatment of community-acquired meticillin-resistant Staphylococcus aureus skin and soft-tissue infections. Int J Antimicrob Agents. 2013;42(6):497–9.
59. Cunha BA. Minocycline is a reliable and effective oral option to treat meticillin-resistant Staphylococcus aureus skin and soft-tissue infections, including doxycycline treatment failures. Int J Antimicrob Agents. 2014;43(4):386–7.
60. Fu Y, Kao WJ. Drug release kinetics and transport mechanisms from semi-interpenetrating networks of gelatin and poly (ethylene glycol) diacrylate. Pharm Res. 2009;26(9):2115–24.
61. Josef E, Barat K, Barsht I, Zilberman M, Bianco-Peled H. Composite hydrogels as a vehicle for releasing drugs with a wide range of hydrophobicities. Acta Biomater. 2013;9(11):8815–22.
62. Jordan J, Fernandez-Gomez FJ, Ramos M, Ikuta I, Aguirre N, Galindo MF. Minocycline and cytoprotection: shedding new light on a shadowy controversy. Curr Drug Deliv. 2007;4(3):225–31.